PERGAMON

Atmospheric Environment 34 (2000) 117–137

ATMOSPHERIC ENVIRONMENT

www.elsevier.com/locate/atmosenv

A comparative review of inorganic aerosol thermodynamic equilibrium modules: similarities, differences, and their likely causes

Yang Zhang[a,*], Christian Seigneur[a], John H. Seinfeld[b], Mark Jacobson[c], Simon L. Clegg[d], Francis S. Binkowski[e]

[a]*Atmospheric & Environmental Research, Inc., 2682 Bishop Drive, Suite 120, San Ramon, CA 94583, USA*
[b]*California Institute of Technology, Pasadena, CA 91125, USA*
[c]*Stanford University, Stanford, CA 94305, USA*
[d]*University of East Anglia, Norwich NR4 7TJ, UK*
[e]*National Oceanic and Atmospheric Administration, On assignment to the US Environmental Protection Agency, Research Triangle Park, NC 27711, USA*

Received 1 December 1998; accepted 26 April 1999

Abstract

A comprehensive comparison of five inorganic aerosol thermodynamic equilibrium modules, MARS-A, SEQUILIB, SCAPE2, EQUISOLV II, and AIM2, was conducted for a variety of atmospheric concentrations of particulate matter (PM) constituents, relative humidities (RHs), and temperatures. Our results show that although the PM compositions and concentrations predicted by these modules are generally comparable under most conditions, significant discrepancies exist under some conditions, especially at high nitrate/chloride concentrations and low/medium RHs. As a consequence, the absolute differences in total PM concentrations predicted by these modules under all simulation conditions are 7.7–12.3% on average and as much as 68% for specific cases. The PM predictions are highly sensitive to changes in the molar ratios of ammonium to sulfate, nitrate to sulfate, and sodium chloride to sulfate, relative humidity, and temperature. The similarities and differences in simulation results predicted by the five modules are analyzed and the likely causes for these differences are discussed in detail. Recommendations are provided regarding the relative advantages of these modules, possible improvements of their performance, and applications in three-dimensional PM modeling studies.

Keywords: Inorganic particulate matter; Thermodynamic modeling; Multi-phase equilibrium; Module comparison; Sensitivity

1. Introduction

Particulate matter (PM) is an ubiquitous component of the atmosphere and plays an important role in many areas of atmospheric sciences including human health effects of air pollution, atmospheric visibility reduction, acid deposition, and the earth's radiation budget. The US Environmental Protection Agency (EPA) revised the National Ambient Air Quality Standards for PM in 1997 to protect human health and has recently proposed new regulations to protect atmospheric visibility. The radiative forcing of aerosols is now routinely included in climate studies. Atmospheric PM models are effective tools to quantify the relationship between sources of air pollutants and their health and environmental impacts. An essential component of the PM models is the thermodynamic module that simulates the partitioning of chemical species among the gas, aqueous, and solid phases and predicts the total mass and chemical composition of PM.

* Corresponding author. Fax: +1-925-244-7129.
E-mail address: yzhang@aer.com (Y. Zhang)

1352-2310/99/$ - see front matter
PII: S1352-2310(99)00236-8

Atmospheric PM consists of inorganic and organic species such as sulfate, nitrate, chloride, water content, soil dust, elemental carbon, and organic carbon. Some of them are emitted directly into the atmosphere (primary PM), whereas others are formed in the atmosphere from the reactions of gases (secondary PM). Inorganic and organic compounds roughly comprise 25–50% and 40–65% of fine particle mass, respectively (Gray et al., 1986). Considerable effort has been directed toward an understanding of the physical and chemical properties of inorganic aerosols and several inorganic aerosol thermodynamic modules have been developed during the past two decades. Such modules include EQUIL (Bassett and Seinfeld, 1983), KEQUIL (Bassett and Seinfeld, 1984), MARS (Saxena et al., 1986), SEQUILIB (Pilinis and Seinfeld, 1987), SCAPE and SCAPE2 (Kim et al., 1993a,b; Kim and Seinfeld, 1995; Meng et al., 1995), MARS-A (Binkowski and Shankar, 1995), EQUISOLV and EQUISOLV II (Jacobson et al., 1996a; Jacobson, 1999a,b), AIM and AIM2 (Wexler and Seinfeld, 1990,1991; Clegg et al., 1992,1994,1995,1998a,b), ISORROPIA (Nenes et al., 1998,1999), and GFEMN (Ansari and Pandis, 1999a). All these modules simulate internally mixed particles, i.e., all particles simulated in a given particle size range have the same composition. Most modules assume that thermodynamic equilibrium exists between the gas and particulate phases for the volatile compounds. Non-equilibrium between the bulk gas phase and the particles has been suggested by some observations (Allen et al., 1989) and non-equilibrium conditions involving mass transport between the bulk gas and particulate phases have been simulated with AIM, SCAPE2, and EQUISOLV/EQUISOLV II. Modeling of secondary organic aerosol (SOA) formation and thermodynamics is more difficult due mainly to major uncertainties in the gas-phase chemistry of SOA formation, phase-partitioning of the condensable organic gases, and thermodynamics of organic PM. Among these modules, only SCAPE2 and EQUISOLV/EQUISOLV II include simple thermodynamic treatments for a few organic compounds.

We focus here on the treatment of the thermodynamic equilibrium of inorganic species and present a quantitative evaluation of five thermodynamic equilibrium modules that are currently used in three-dimensional (3-D) air quality PM models. The comparison is performed in stand-alone modes (i.e., outside of their 3-D host air quality models) to eliminate the influence of other atmospheric processes (e.g., gas-phase chemistry and transport) treated in these 3-D host models. Thus, the differences in PM predictions among these modules are due solely to the differences in the model formulations and/or numerical algorithms. The modules selected for comparison include MARS-A, SEQUILIB, SCAPE2, EQUISOLV II, and AIM2. We initially used EQUISOLV for this comparison and identified that under some conditions the numerical solution did not converge. In conjunction with this work, an improved version of EQUISOLV, i.e., EQUISOLV II, was then developed (Jacobson, 1999b) and used for the rest of this study. MARS-A is used in EPA Models-3 (Binkowski and Shankar, 1995) and the Denver Air Quality Model, DAQM (Middleton, 1997). SEQUILIB is used in SAQM-AERO (Dabdub et al., 1997) and UAM-AERO (Lurmann et al., 1997). SCAPE2 is used in the CIT model (Meng et al., 1998). EQUISOLV II is used in GATOR (Jacobson et al., 1996b; Jacobson, 1997). A revised version of AIM has been incorporated in UAM-IV (Sun and Wexler, 1998).

Our objectives are to gain an understanding of the relative strengths and weaknesses of each thermodynamic equilibrium module by comparing the module predictions under a variety of thermodynamic regimes, to suggest further improvements of their performance, and to provide recommendations for the selection of such modules for applications in future 3-D PM modeling studies. The particle size distribution and size-resolved chemical equilibrium are not taken into account in this comparison.

2. Description of thermodynamic equilibrium modules

Tables 1 and 2 summarize the major characteristics of the five thermodynamic modules and the equilibria included in these modules, respectively. All five modules simulate the partitioning of chemical species among gas, aqueous, and solid phases. However, there are major differences in many aspects of the module formulations. These differences will be described in detail along with the discussion of results in Section 3.3. There are three versions of AIM2. AIM2-Model I simulates the H^+–SO_4^{2-}–NO_3^-–Cl^-–Br^-–H_2O system under stratospheric conditions for temperatures from less than 200–328 K; AIM2-Model II simulates the H^+–NH_4^+–SO_4^{2-}–NO_3^-–H_2O system under tropospheric conditions at any tropospheric temperatures; and AIM2-Model III simulates the H^+–NH_4^+–Na^+–SO_4^{2-}–NO_3^-–Cl^-–H_2O system under tropospheric conditions and is restricted to 298.15 K only. AIM2-Model III is used in this study and is referred to as AIM2.

3. Comparison of simulation results

3.1. Simulation conditions and comparison procedures

The five modules were run for 20 different sets of initial compositions, as listed in Table 3. These compositions cover most of the expected range of thermodynamic equilibrium regimes under typical urban and coastal atmospheric conditions. For each condition, we conducted 10 simulations using 10 different RHs ranging from 10 to 95% for 298.15 K. The simulations were repeated for 308.15 K (except for AIM2). Although SCAPE2 and

Table 1
Major characteristics of MARS-A, SEQUILIB, SCAPE2, EQUISOLV II, and AIM2

	MARS-A	SEQUILIB	SCAPE2	EQUISOLV II	AIM2
Chemical species treated in the thermodynamic equilibrium calculations[a]	Sulfate, nitrate, ammonium, water	Sulfate, nitrate, ammonium, sodium, chloride, water	Sulfate, nitrate, ammonium, chloride, sodium, potassium, calcium, magnesium, carbonate, water	Sulfate, nitrate, ammonium, chloride, sodium, potassium, calcium, magnesium, carbonate, water	Sulfate, nitrate, ammonium, sodium, chloride, eight complex salts of ammonium and sodium, water
Activity coefficients[b]	Pitzer method for binary activity coefficients. Bromley method for multi-component activity coefficients	Pitzer method for binary activity coefficients. Bromley method for multi-component activity coefficients	Kusik–Meissner method for binary activity coefficients. Option of using Bromley, Kusik–Meissner or Pitzer methods for multi-component activity coefficients. Zdanovskii, Robinson and Stokes (ZSR) method for water activity	A number of sources such as Hamer and Wu, Goldberg, Bassett and Seinfeld, Filippov et al. and Pitzer methods for binary activity coefficients. Bromley method for multi-component activity coefficients	Pitzer, Simonson and Clegg method for multicomponent activity coefficients and water activities using mole fraction based electrolyte thermodynamic model
Temperature dependence	Equilibrium constants	Equilibrium constants	Equilibrium constants, DRHs	Equilibrium constants, DRHs, and activity coefficients	See note[c]
Method used to obtain solution to thermodynamic equilibrium	Analytical	Bisectional and Newton–Raphson	Bisectional	Mass flux iteration (MFI) and analytical equilibrium iteration (AEI)	Minimization of the Gibbs free energy of the system using sequential quadratic programming algorithm
References[d]	Saxena et al. (1986) and Binkowski and Shankar (1995)	Pilinis and Seinfeld (1987)	Kim et al. (1993a,b), Kim and Seinfeld (1995) and Meng et al. (1995)	Jacobson et al. (1996a) and Jacobson (1999a,b)	Clegg et al. (1992,1994,1995,1998a,b)

[a] Other species that are soluble in water are also included through their Henry's law equilibrium constant, however, they do not interact with the other species in the thermodynamic equilibrium calculation. For example, several organic and inorganic compounds in EQUISOLV II. SCAPE2 considers interactions of formate and acetate with other ionic species, but this treatment is not included in the current release of the model.

[b] The Pitzer method for multicomponent activity coefficients does not require estimation of binary activity coefficients.

[c] AIM2-Models I and II (for H^+, NO_3^-, SO_4^{2-}, Cl^-, Br^-, H_2O and H^+, NH_4^+, NO_3^-, SO_4^{2-}, H_2O, respectively) account for temperature-dependence of all modeled properties including equilibrium constants, chemical potentials, DRHs, activities, solubilities, and freezing points. The version of AIM2 (i.e., AIM2-Model III) used for this comparison is valid for the system H^+, NH_4^+, Na^+, NO_3^-, SO_4^{2-}, Cl^-, H_2O and is restricted to 298.15 K only.

[d] References pertain to published information, subsequent modifications have been made to some modules.

Table 2
Chemical equilibrium reactions included in MARS-A, SEQUILIB, SCAPE2, EQUISOLV II, and AIM2

Equilibrium reaction	Equilibrium constant[a,b]							
	K (298.15)	a	b	MARS-A	SEQUILIB	SCAPE2	EQUISOLV II	AIM2[m]
E1 $H_2SO_4(aq) = H^+(aq) + HSO_4^-(aq)$	1.0×10^{3}[d]	—	—				✓	
E2 $HSO_4^-(aq) = H^+(aq) + SO_4^{2-}(aq)$	1.015×10^{-2}[e]	8.85	25.14	✓	✓	✓	✓	✓
E3 $NH_3(g) = NH_3(aq)$	5.7639×10^{1}	13.79	− 5.393	✓		✓	✓[c]	
E4a $NH_3(aq) + H_2O(l) = NH_4^+(aq) + OH^-(aq)$	1.805×10^{-5}	− 1.50	26.92	✓		✓	✓[c]	
E4b $NH_3(g) + H^+(aq) = NH_4^+(aq)$	1.0677×10^{11}[d]	—	—					✓
E5 $HCl(g) = H^+(aq) + Cl^-(aq)$	1.971×10^{6}	30.20	19.91		✓	✓	✓	✓
E6 $HNO_3(g) = H^+(aq) + NO_3^-(aq)$	2.511×10^{6}[f]	29.17	16.83	✓	✓	✓	✓	✓
E7 $H_2O(l) = H^+(aq) + OH^-(aq)$	1.010×10^{-14}	− 22.52	26.92	✓	✓	✓	✓	
E8 $Na_2SO_4(s) = 2Na^+(aq) + SO_4^{2-}(aq)$	4.799×10^{-1}	0.98	39.75		✓	✓	✓	✓
E9 $NH_4Cl(s) = NH_3(g) + HCl(g)$	1.086×10^{-16}	− 71.00	2.40		✓	✓	✓[c]	✓
E10 $(NH_4)_2SO_4(s) = 2NH_4^+(aq) + SO_4^{2-}(aq)$	1.817[g]	− 2.65	38.57		✓	✓	✓	✓
E11 $NaCl(s) = Na^+(aq) + Cl^-(aq)$	3.7661×10^{1}	− 1.56	16.90		✓	✓	✓	✓
E12 $NaNO_3(s) = Na^+(aq) + NO_3^-(aq)$	1.1977×10^{1}	− 8.22	16.01		✓	✓	✓	✓
E13 $NH_4NO_3(s) = NH_3(g) + HNO_3(g)$	5.746×10^{-17}[h]	− 74.38	6.12	✓	✓	✓	✓[c]	✓
E14 $NaHSO_4(s) = Na^+(aq) + HSO_4^-(aq)$	2.413×10^{4}[i]	0.79	14.746		✓	✓	✓	✓
E15 $NH_4HSO_4(s) = NH_4^+(aq) + HSO_4^-(aq)$	2.55×10^{2}[j]	− 2.87	15.83			✓	✓	✓
E16 $(NH_4)_3H(SO_4)_2(s) = 3NH_4^+(aq) + HSO_4^-(aq) + SO_4^{2-}(aq)$	4.0026×10^{1}[k]	− 5.19	54.40			✓	✓	✓
E17 $NH_4Cl(s) = NH_4^+(aq) + Cl^-(aq)$	2.205×10^{1}[d]	− 5.95	16.91				✓	✓
E18 $NH_4NO_3(s) = NH_4^+(aq) + NO_3^-(aq)$	1.4863×10^{1}[d]	− 10.364	17.561				✓	✓
E19 $NH_3(g) + HNO_3(g) = NH_4^+(aq) + NO_3^-(aq)$	2.587×10^{17}[d,l]	64.02	11.44	✓	✓		✓	✓
E20 $NH_3(g) + HCl(g) = NH_4^+(aq) + Cl^-(aq)$	2.025×10^{17}[d]	65.05	14.51		✓		✓[c]	✓
E21 $NaCl(s) + HNO_3(g) = NaNO_3(s) + HCl(g)$	4.008[d]	5.63	− 2.19		✓		✓[c]	✓
E22 $Na_3H(SO_4)_2(s) = 3Na^+(aq) + HSO_4^-(aq) + SO_4^{2-}(aq)$	1.7939×10^{1}[d]	—	—					✓
E23 $(NH_4)_2SO_4 \cdot 2NH_4NO_3(s) = 4NH_4^+(aq) + SO_4^{2-}(aq) + 2NO_3^-(aq)$	8.5030×10^{1}[d]	—	—					✓
E24 $(NH_4)_2SO_4 \cdot 3NH_4NO_3(s) = 5NH_4^+(aq) + SO_4^{2-}(aq) + 3NO_3^-(aq)$	8.8020×10^{2}[d]	—	—					✓
E25 $NH_4HSO_4 \cdot NH_4NO_3(s) = 2NH_4^+(aq) + HSO_4^-(aq) + NO_3^-(aq)$	1.2792×10^{3}[d]	—	—					✓
E26 $Na_2SO_4 \cdot 10H_2O(s) = 2Na^+(aq) + SO_4^{2-}(aq) + 10H_2O(l)$	5.9666×10^{-2}[d]	—	—					✓
E27 $Na_2SO_4 \cdot NaNO_3 \cdot H_2O(s) = 3Na^+(aq) + SO_4^{2-}(aq) + NO_3^-(aq) + H_2O(l)$	8.0592×10^{-1}[d]	—	—					✓
E28 $NaHSO_4 \cdot H_2O(s) = Na^+(aq) + HSO_4^-(aq) + H_2O(l)$	7.5206×10^{1}[d]	—	—					✓
E29 $NaH_3(SO_4)_2 \cdot H_2O(s) = Na^+(aq) + 2HSO_4^-(aq) + H^+(aq) + H_2O(l)$	5.9121×10^{8}[d]	—	—					✓
E30 $Na_2SO_4(NH_4)_2SO_4 \cdot 4H_2(s) = 2Na^+(aq) + 2SO_4^{2-}(aq) + 2NH_4^+(aq) + 4H_2O(l)$	2.0284×10^{-2}[d]	—	—					✓
E31 $KCl(s) = K^+(aq) + Cl^-(aq)$	8.680	− 6.901	19.95			✓[c]	✓[c]	
E32 $K_2SO_4(s) = 2K^+(aq) + SO_4^{2-}(aq)$	1.569×10^{-2}	− 9.585	45.81			✓[c]	✓[c]	
E33 $KHSO_4(s) = K^+(aq) + HSO_4^-(aq)$	2.4016×10^{1}	− 8.428	17.97			✓[c]	✓[c]	
E34 $KNO_3(s) = K^+(aq) + NO_3^-(aq)$	8.72×10^{-1}	− 14.07	19.38			✓[c]	✓[c]	
E35 $CaCl_2(s) = Ca^{2+}(aq) + 2Cl^-(aq)$	7.974×10^{11}	—	—			✓[c]	✓[c]	
E36 $CaSO_4 \cdot 2H_2O(s) = Ca^{2+}(aq) + SO_4^{2-}(aq) + 2H_2O(l)$	4.319×10^{-5}	—	—			✓[c]	✓[c]	

E37 $Ca(NO_3)_2(s) = Ca^{2+}(aq) + 2NO_3^-(aq)$	6.607×10^5	—	—	✓[e]	✓[e]
E38 $MgCl_2(s) = Mg^{2+}(aq) + 2Cl^-(aq)$	9.557×10^{21}	—	—	✓[e]	✓[e]
E39 $MgSO_4(s) = Mg^{2+}(aq) + SO_4^{2-}(aq)$	1.079×10^5	—	—	✓[e]	✓[e]
E40 $Mg(NO_3)_2(s) = Mg^{2+}(aq) + 2NO_3^-(aq)$	2.507×10^{15}	—	—	✓[e]	✓[e]
E41 $CO_2(g) = CO_2(aq)$	3.404×10^{-2}	8.1858	− 28.9307	✓[e]	✓[e]
E42 $CO_2(aq) + H_2O(l) = HCO_3^-(aq) + H^+(aq)$	4.299×10^{-7}	− 3.0821	31.8139	✓[e]	✓[e]
E43 $HCO_3^-(aq) = H^+(aq) + CO_3^{2-}(aq)$	4.678×10^{-11}	− 5.9908	38.8440	✓[e]	✓[e]
E44 $NH_3(aq) + HCO_3^- = NH_2CO_2^-(aq) + H_2O(l)$	3.0424	9.7119	—	✓[e]	
E45 $Na_2CO_3(s) = 2Na^+(aq) + CO_3^{2-}(aq)$	1.811×10^1	10.7713	30.5533	✓[e]	✓[e]
E46 $NaHCO_3(s) = Na^+(aq) + HCO_3^-(aq)$	3.914×10^{-1}	− 7.5439	− 5.6796	✓[e]	✓[e]
E47 $K_2CO_3(s) = 2K^+(aq) + CO_3^{2-}(aq)$	2.541×10^5	12.4575	36.7272	✓[e]	✓[e]
E48 $KHCO_3(s) = K^+(aq) + HCO_3^-(aq)$	1.399×10^1	− 7.5964	− 2.5210	✓[e]	✓[e]
E49 $CaCO_3$(calcite, s) $= Ca^{2+}(aq) + CO_3^{2-}(aq)$	4.959×10^{-9}	—	—	✓[e]	✓[e]
E50 $MgCO_3(s) = Mg^{2+}(aq) + CO_3^{2-}(aq)$	6.812×10^{-6}	—	—	✓[e]	✓[e]
E51 $NH_2COONH_4(s) = NH_2CO_2^-(aq) + NH_4^+(aq)$	6.4023×10^1	—	—	✓[e]	

[a] The subscripts *g*, *aq*, *l*, and *s* in the equilibrium reactions represent concentrations of the species in the gas, the aqueous, the liquid, and the solid phases, respectively. Equilibrium constants are expressed as:

$$K(T) = K(T_0)\exp\left\{a\left(\frac{T_0}{T} - 1\right) + b\left(1 + \ln\left(\frac{T_0}{T}\right) - \frac{T_0}{T}\right)\right\}, \text{ where } T_0 = 298.15\ \text{K}$$

The values of equilibrium constants are those used in SCAPE2 except otherwise indicated. The equilibrium constants used in the other modules are the same as or similar to those of SCAPE2 except otherwise indicated.

[b] The units for equilibrium constants are:

$A(aq) = B(aq) + C(aq)\ \text{mol kg}^{-1}$

$A(g) = xB(aq) + yC(aq)\ \text{mol}^{(x+y)}\ \text{kg}^{-(x+y)}\ \text{atm}^{-1}$

$A(s) = B(g) + C(g)\ \text{atm}^2$

$A(s) = xB(aq) + yC(aq) + zD(aq)\ \text{mol}^{(x+y+z)}\ \text{kg}^{-(x+y+z)}$

$A(g) + B(g) = C(aq) + D(aq)\ \text{mol}^2\ \text{kg}^{-2}\ \text{atm}^{-2}$

$A(aq) + B(aq) = C(aq)\ \text{kg mol}^{-1}$

[c] The equilibrium reactions are included in the original module formulation but not used for the base simulations in this work.

[d] The equilibrium constants for E1 and E17 − E21 are those used in EQUISOLV II. The equilibrium constants for E4b and E22-E30 are those used in AIM2.

[e] The values of K, a, and b for E2 are 1.031×10^{-2}, 7.59, and 18.825 in SEQUILIB, respectively.

[f] The values of K, a, and b for E6 are 3.638×10^6, 29.47, and 16.835 in SEQUILIB, respectively.

[g] The values of K, a, and b for E10 are 1.425, − 2.65, and 38.55 in SEQUILIB, respectively.

[h] The values of K, a, and b for E13 are 2.986×10^{-17}, − 75.108, and 13.456 in SEQUILIB, and 4.1994×10^{-17}, − 74.7531, and 6.025 in MARS-A, respectively.

[i] The values of K, a, and b for E14 are 2.44×10^4, 0.79, and 4.53 in SEQUILIB, respectively.

[j] The values of K, a, and b for E15 are 1.383×10^2, − 2.87, and 15.83 in EQUISOLV II, respectively.

[k] The values of K, a, and b for E16 are 2.926×10^1, − 5.19, and 54.40 in EQUISOLV II, respectively.

[l] The values of K, a, and b for E19 are 2.5865×10^{17}, 63.98, and 11.44 in MARS-A, and 3.999×10^{17}, 64.698, and 11.505 in SEQUILIB, respectively.

[m] The version of AIM2 used in this work is restricted to 298.15 K only. AIM2 does not work in terms of equilibrium constants. The values of K(298.15) were computed based on the Gibbs energies of formation used in AIM2.

Table 3
List of conditions for thermodynamic equilibrium module simulations[a]

Initial compositions	Total ammonium/sulfate mole ratio	Total nitrate/sulfate mole ratio	Total sodium chloride/sulfate mole ratio
1	0.5	1.0	0
2	1.0	1.0	0
3	1.5	1.0	0
4	2.0	1.0	0
5	4.0	1.0	0
6	1.5	0.33	0
7	4.0	0.33	0
8	1.5	3.0	0
9	4.0	3.0	0
10	0.5	1.0	0.5
11	1.0	1.0	0.5
12	1.5	1.0	0.5
13	2.0	1.0	0.5
14	4.0	1.0	0.5
15	1.5	0.33	0.5
16	4.0	0.33	0.5
17	1.5	3.0	0.5
18	4.0	3.0	0.5
19	1.5	1.0	2.0
20	4.0	1.0	2.0

[a]Particulate sulfate concentration is 20 μg m^{-3} for all initial compositions. Simulations under each set of initial compositions were conducted for 10, 20, 30, 40, 50, 60, 70, 80, 90 and 95% relative humidity (RH) and temperatures of 298.15 and 308.15 K.

EQUISOLV II treat potassium, calcium, magnesium, and carbonate, these species are not included here. The hysteresis and the Kelvin effects can be simulated in SCAPE2, EQUISOLV II, and AIM2, however, they are not considered in this study.

For the 20 conditions, the concentration of total sulfate is set to be a constant value of 20 μg m^{-3}. H_2SO_4 has a very low vapor pressure; consequently, it is present solely in the particulate phase and its concentration is used as a reference for the other species. For the purpose of this analysis, we define the initial atmospheric chemical concentrations according to the following four dimensionless ratios: the molar ratio of total ammonium (i.e., sum of gaseous ammonia, NH_3(g), and particulate ammonium, NH_4^+(p)) to total sulfate (referred to as TNH_4/TSO_4), the molar ratio of total nitrate (i.e., sum of gaseous nitric acid, HNO_3(g), and particulate nitrate, NO_3^-(p)) to total sulfate (referred to as TNO_3/TSO_4), the molar ratio of total sodium chloride to total sulfate (referred to as $TNaCl/TSO_4$), and the molar ratio of total cation species (i.e., sum of total ammonium, TNH_4, and total sodium, TNa) to total sulfate (referred to as $TCAT/TSO_4$). The particulate phase concentrations of ammonium, nitrate, and chloride (i.e., NH_4^+(p), NO_3^-(p), and Cl^-(p)) include their concentrations in the solid and aqueous phases. If $TCAT/TSO_4 < 2$, the system contains excess sulfate and is called sulfate-rich. If $TCAT/TSO_4 = 2$, the system contains just sufficient sulfate to neutralize the cation species and is called sulfate-neutral. If $TCAT/TSO_4 > 2$, the system does not contain enough sulfate to neutralize the cation species and is called sulfate-poor. For the 20 sets of conditions, conditions 1–3, 6, 8, 10, and 11 are sulfate-rich, conditions 4, 12, 15, and 17 are sulfate-neutral, and conditions 5, 7, 9, 13, 14, 16, and 18–20 are sulfate-poor.

A synoptic comparison of the simulation results is provided in Section 3.2. The similarities and differences in the model predictions for different thermodynamic regimes as well as the likely causes are presented and analyzed in detail in Section 3.3. In our comparisons, SCAPE2 was used as the reference for MARS-A and SEQUILIB since it contains more chemical species and equilibrium reactions and offers more detailed aerosol thermodynamic calculations than MARS-A and SEQUILIB. Since SCAPE2, EQUISOLV II, and AIM2 contain the similar detailed level of chemistry and thermodynamics, we compare results between SCAPE2 and EQUISOLV II, between SCAPE2 and AIM2, and between EQUISOLV II and AIM2. For each pair of these three modules, we use the arithmetic average values predicted by each pair as reference.

3.2. Synoptic comparisons

Fig. 1 shows concentrations of total particulate phase concentrations of nitrate, ammonium, hydrogen ion,

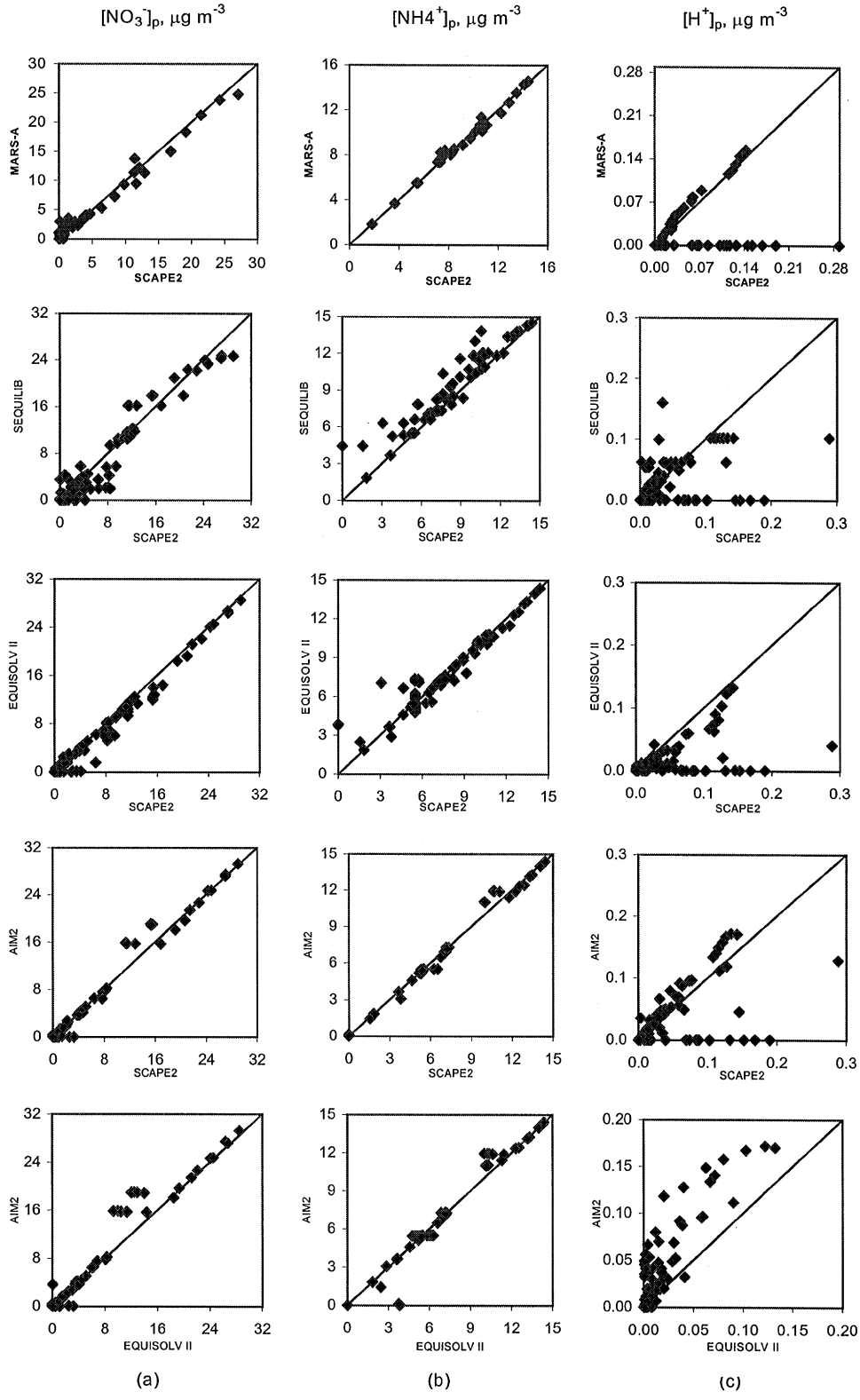

Fig. 1. A synoptic comparison of concentrations of total particulate-phase concentrations of (a) nitrate, (b) ammonium, (c) hydrogen ion, (d) chloride, (e) water, and (f) total PM predicted by the five chemical equilibrium modules under all simulation conditions shown in Table 2 and a temperature of 298.15 K.

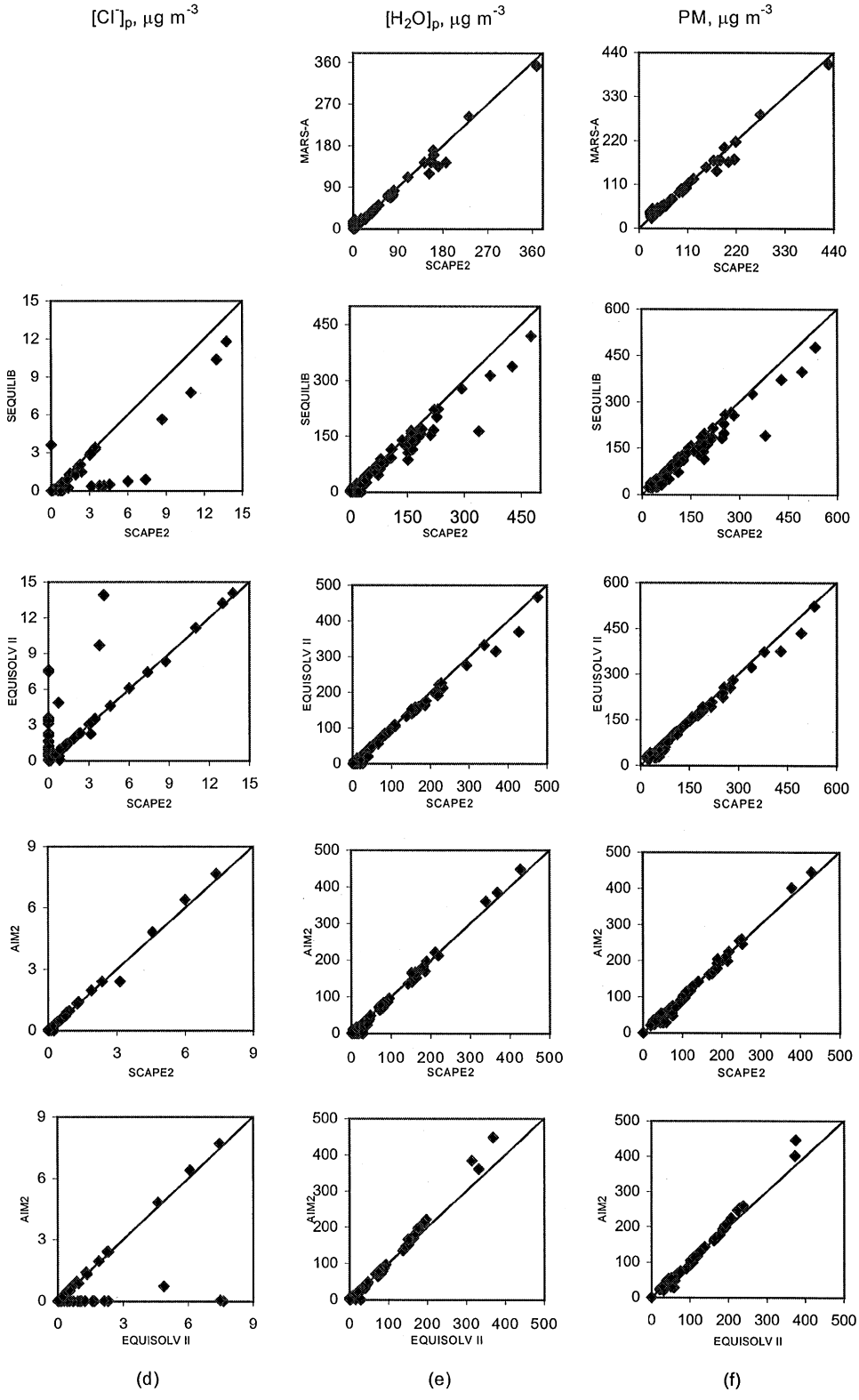

Fig. 1. (*Continued*).

chloride, water, and total PM (labeled as $[NO_3^-]_p$, $[NH_4^+]_p$, $[H^+]_p$, $[Cl^-]_p$, $[H_2O]_p$, and PM) predicted by the five modules under all simulation conditions. For comparisons between MARS-A and SCAPE2, only 90 cases were used because MARS-A does not simulate systems containing NaCl. For comparisons between AIM2 and SCAPE2 or EQUISOLV II, only 150 cases were used because 50 of 200 cases are alkaline and AIM2 does not simulate such cases. $[NO_3^-]_p$, $[NH_4^+]_p$, $[H_2O]_p$, and total PM concentrations predicted by these modules are generally comparable, but there are significant discrepancies in the predictions of $[H^+]_p$ and $[Cl^-]_p$.

3.2.1. Particulate nitrate

Under most conditions, $[NO_3^-]_p$ predicted by MARS-A, SCAPE2, EQUISOLV II, and AIM2 are similar to each other, whereas SEQUILIB shows significant deviations from SCAPE2, as shown in Fig. 1(a). All modules predict either zero or negligible amounts of NO_3^-(p) for RH < 30–70% (except in a few cases with high ammonium and nitrate). Under higher RH conditions, MARS-A predicts slightly higher $[NO_3^-]_p$ than SCAPE2 for $TNH_4/TSO_4 \leqslant 2$ and lower $[NO_3^-]_p$ than SCAPE2 for $TNH_4/TSO_4 = 4$. Differences in the $[NO_3^-]_p$ predicted by MARS-A and SCAPE2 are mainly due to simplified chemistry and thermodynamic calculations used in MARS-A for NO_3^-(p). SEQUILIB predicts significantly higher $[NO_3^-]_p$ than SCAPE2 for most cases with $TNH_4/TSO_4 = 1.5$ and 4, but it predicts significantly lower $[NO_3^-]_p$ than SCAPE2 for $TNH_4/TSO_4 = 1$, and zero $[NO_3^-]_p$ for some cases with $TNH_4/TSO_4 = 0.5$ and 2 even under high RH conditions. SCAPE2 and EQUISOLV II predict similar $[NO_3^-]_p$ for all cases with $TNH_4/TSO_4 \leqslant 2$ and RH $> 70\%$. However, $[NO_3^-]_p$ predicted by SCAPE2 are significantly higher than that predicted by EQUISOLV II for some cases with high ammonium and medium RHs due to different $NH_3(g)/NH_4^+$ equilibria treated in the two modules (see Section 3.3.1). $[NO_3^-]_p$ predicted by AIM2 are similar to that predicted by SCAPE2 and EQUISOLV II for most acidic cases. For some cases with low RHs and high ammonium and nitrate, however, AIM2 predicts higher $[NO_3^-]_p$ than SCAPE2 and EQUISOLV II. This is because AIM2 simulates a different chemistry involving complex salts such as $2\ NH_4NO_3 \cdot (NH_4)_2SO_4$ and uses a different method for calculations of multi-component activity coefficients.

3.2.2. Particulate ammonium

$[NH_4^+]_p$ predicted by MARS-A, SCAPE2, EQUISOLV II, and AIM2 are in good agreement under most conditions, as shown in Fig. 1(b). SEQUILIB predicts $[NH_4^+]_p$ deviating within 14% of that predicted by SCAPE2 for all cases without NaCl, but it predicts significantly higher $[NH_4^+]_p$ (up to 37%) than SCAPE2 for many cases with NaCl and/or $TCAT/TSO_4 > 2$, due to more formation of NH_4NO_3 or NH_4Cl, or both predicted by SEQUILIB under these conditions. Significant differences in $[NH_4^+]_p$ predicted by SCAPE2 and EQUISOLV II are found for some cases with high ammonium and low nitrate regardless of the presence of NaCl. Out of these cases, $[NH_4^+]_p$ predicted by EQUISOLV II are lower than those predicted by SCAPE2 in the absence of NaCl and the results become just the opposite in the presence of NaCl due to different sets of $NH_3(g)/NH_4^+$ equilibria used in both modules. For most acidic cases, $[NH_4^+]_p$ predicted by SCAPE2 and EQUISOLV II are similar to those predicted by AIM2. $[NH_4^+]_p$ predicted by AIM2 are higher than those predicted by SCAPE2 and EQUISOLV II for a few cases with high ammonium and nitrate.

3.2.3. Particulate hydrogen ion

Fig. 1(c) shows $[H^+]_p$ predicted by the five modules. Significant discrepancies exist because of either some assumptions related to H^+(p) calculations used in MARS-A and SEQUILIB or the different numerical methods used to calculate H^+(p). For example, MARS-A and SEQUILIB assume $[H^+]_p$ to be zero for all cases with $TCAT/TSO_4 > 2$ and $TCAT/TSO_4 \geqslant 2$, respectively, thus no H^+(p) concentrations are computed for these cases in the two modules. For some sulfate-rich and low RH cases, MARS-A also predicts $[H^+]_p$ to be zero. For many sulfate rich and low RH cases (i.e., $TCAT/TSO_4 < 2$ and RH $< 70\%$), $[H^+]_p$ predicted by SCAPE2 are significantly higher than those predicted by other modules because of non convergence of the solutions in SCAPE2. For most cases with high RHs, all modules predict similar $[H^+]_p$ except SEQUILIB which sometimes predicts either zero or abnormally higher $[H^+]_p$. In most cases, the aqueous particle predicted by SCAPE2 is more acidic than that predicted by EQUISOLV II. In most cases, $[H^+]_p$ predicted by SCAPE2 are either higher or slightly lower than those predicted by AIM2, and $[H^+]_p$ predicted by EQUISOLV II are lower than those predicted by AIM2.

3.2.4. Particulate chloride

Fig. 1(d) shows that there are substantial differences in $[Cl^-]_p$ predicted by SEQUILIB, SCAPE2, EQUISOLV II, and AIM2. For most cases with RH $> 50\%$, AIM2, SCAPE2, and EQUISOLV II predict similar $[Cl^-]_p$, whereas SEQUILIB predicts significantly lower $[Cl^-]_p$ than those predicted by the other modules. For most cases with RH $< 50\%$, SEQUILIB, SCAPE2, and AIM2 predict no $[Cl^-]_p$. On the other hand, in most of these cases, EQUISOLV II predicts the co-existence of solid NH_4Cl(s) and NaCl(s), resulting in significantly higher $[Cl^-]_p$ than those predicted by the other three modules. SCAPE2 and AIM2 include similar sets of reactions for NH_4Cl and NH_4NO_3 and predict comparable $[Cl^-]_p$.

The different results of SEQUILIB and EQUISOLV II are due mainly to the fact that the two modules include different sets of equilibrium reactions for NH_4Cl and NH_4NO_3.

3.2.5. Particulate water content

For most conditions, $[H_2O]_p$ predicted by the five modules agree well except that SEQUILIB tends to predict lower $[H_2O]_p$ under most conditions, as shown in Fig. 1(e). This is because the binary water activity data used in SEQUILIB are different from those used in the other modules. SEQUILIB uses the older binary water activity data of Cohen et al. (1987a,b) for most electrolytes (Pilinis and Seinfeld, 1987), which may be inaccurate for some salts. Whereas SCAPE2, EQUISOLV II, and AIM2 use the most recent and critically assessed water activity data of Chan et al. (1992) and other researchers. The data of Chan et al. (1992) generally result in higher water content than those of Cohen et al. (1987a,b) (Kim et al., 1993).

3.2.6. Total PM concentrations

Although there remain significant discrepancies in the predicted PM compositions, the total PM concentrations predicted by the five modules under all conditions agree remarkably well, except those predicted by SEQUILIB in the high PM concentration range (total PM $> \sim 150\,\mu g\,m^{-3}$), as shown in Fig. 1(f). Under all conditions, the absolute differences are 12.3, 10.8, 9.3, 9.2, and 7.7% on average between MARS-A and SCAPE2, SEQUILIB and SCAPE2, EQUISOLV II and SCAPE2, AIM2 and SCAPE2, and EQUISOLV II and AIM2, respectively. The absolute differences range from 0.1–61, 0–50, 0–67, 0–68, and 0–67% for specific cases for each pair of modules, respectively. Differences in $PM_{2.5}$ and PM_{10} concentrations will be less because of the presence of primary species in PM that are not included in the chemical systems considered here.

3.2.7. Dominant PM compounds

The dominant PM compounds predicted by the five modules are different for many cases. For cases with $TNO_3/TSO_4 = 1$, $TCAT/TSO_4 > 2$, and all RHs, MARS-A predicts $(NH_4)_2SO_4$ and NH_4NO_3 to be dominant; SEQUILIB predicts either $(NH_4)_2SO_4$ and NH_4NO_3 or $(NH_4)_2SO_4$, NH_4NO_3, Na_2SO_4, and NH_4Cl to be dominant; SCAPE2 predicts either $(NH_4)_2SO_4$ alone or $(NH_4)_2SO_4$, NH_4NO_3, Na_2SO_4, and NH_4Cl to be dominant. EQUISOLV II predicts dominant species similar to those of SCAPE2 for low RHs but an additional species, NH_4NO_3, to be dominant for high RHs; and AIM2 predicts no results for most of these cases because it does not simulate alkaline systems. For the acidic systems, AIM2 predicts similar dominant species to those of SCAPE2 for low RHs but both $(NH_4)_2SO_4$ and $Na_2SO_4 \cdot (NH_4)SO_4 \cdot 4H_2O$ to be dominant for most of these cases for RH $\geqslant 50\%$. For cases with $TNO_3/TSO_4 = 1$, $TCAT/TSO_4 \leqslant 2$ and all RHs, MARS-A predicts $(NH_4)_2SO_4$ and NH_4HSO_4 to be dominant, the other modules predict either bisulfate salts (e.g., NH_4HSO_4, $(NH_4)_3H(SO_4)_2$, and $NaHSO_4$), H_2SO_4, or sulfate salts (e.g., $(NH_4)_2SO_4$ and/or Na_2SO_4) or a combination of these to be dominant. A major difference between AIM2 and the other modules is that AIM2 sometimes predicts more complex salts such as $Na_3H(SO_4)_2$, $NaHSO_4 \cdot H_2O$, and $Na_2SO_4 \cdot (NH_4)_2SO_4 \cdot 4H_2O$ to be dominant; such salts are not treated in the other modules.

3.3. Detailed comparisons

3.3.1. The H^+–NH_4^+–NO_3^-–SO_4^{2-}–H_2O system

Sulfate-rich cases. Under sulfate-rich conditions (i.e., $TNH_4/TSO_4 < 2$), sulfate is in excess and the solution is highly acidic due to insufficient neutralization by NH_4^+. Sulfate may exist as H_2SO_4, HSO_4^-, and SO_4^{2-}. Most nitrate remains in the gas phase and most ammonium resides in the particulate phase. Fig. 2 shows $[NO_3^-]_p$, $[NH_4^+]_p$, $[H^+]_p$, and $[H_2O]_p$ predicted by the five modules for $TNH_4/TSO_4 = 1.5$, where sulfate is partially neutralized mainly as $(NH_4)_3H(SO_4)_2$ and some NH_4NO_3 may be formed.

While $[NO_3^-]_p$ are negligible for RH $\leqslant$ 60–70%, they increase significantly with RH for higher RHs. $[NO_3^-]_p$ from all modules agree within 20% for RH $> 90\%$ but differ notably for RH = 60–90% due to differences in chemistry and activity calculations. Both MARS-A and SEQUILIB predict higher $[NO_3^-]_p$ than the other three modules for RH $> 70\%$ but for different reasons. In SEQUILIB, the equilibrium constant for $HNO_3(g) \Leftrightarrow H^+(aq) + NO_3^-(aq)$ is 44% higher than that used in the other four modules (see Table 2). This causes lower $[HNO_3]_g$, thus higher $[NO_3^-]_p$. The higher $[NO_3^-]_p$ predicted by MARS-A is likely caused by its simplified chemistry and/or the quadratic approximation in the calculation of $[NO_3^-]_p$. $[NH_4^+]_p$ predicted by the five modules are in good agreement, with most ammonium residing in the particulate phase. $NH_4^+(p)$ is mainly present as $(NH_4)_2SO_4$ in MARS-A, as $(NH_4)_2SO_4$ and/or $(NH_4)_3H(SO_4)_2$ in SEQUILIB, SCAPE2, and EQUISOLV II, and as a mixture of $(NH_4)_3H(SO_4)_2$ and NH_4HSO_4 or a mixture of $(NH_4)_3H(SO_4)_2$ and $(NH_4)_2SO_4$ in AIM2. SCAPE2 predicts some $[H^+]_p$ for all RHs, on the other hand, the other four modules predict a small $[H^+]_p$ (up to $0.06\,\mu g\,m^{-3}$) for RH $> 70\%$. The high $[H^+]_p$ predicted by SCAPE2 for RH $< 60\%$ result from the non-convergence of the numerical solution for solid calculations. The large differences in predicted $[H^+]_p$ for RH $> 60\%$ are due to differences in the chemical species and equilibrium reactions treated and the methods used to calculate $[H^+]_p$ and the activity coefficients.

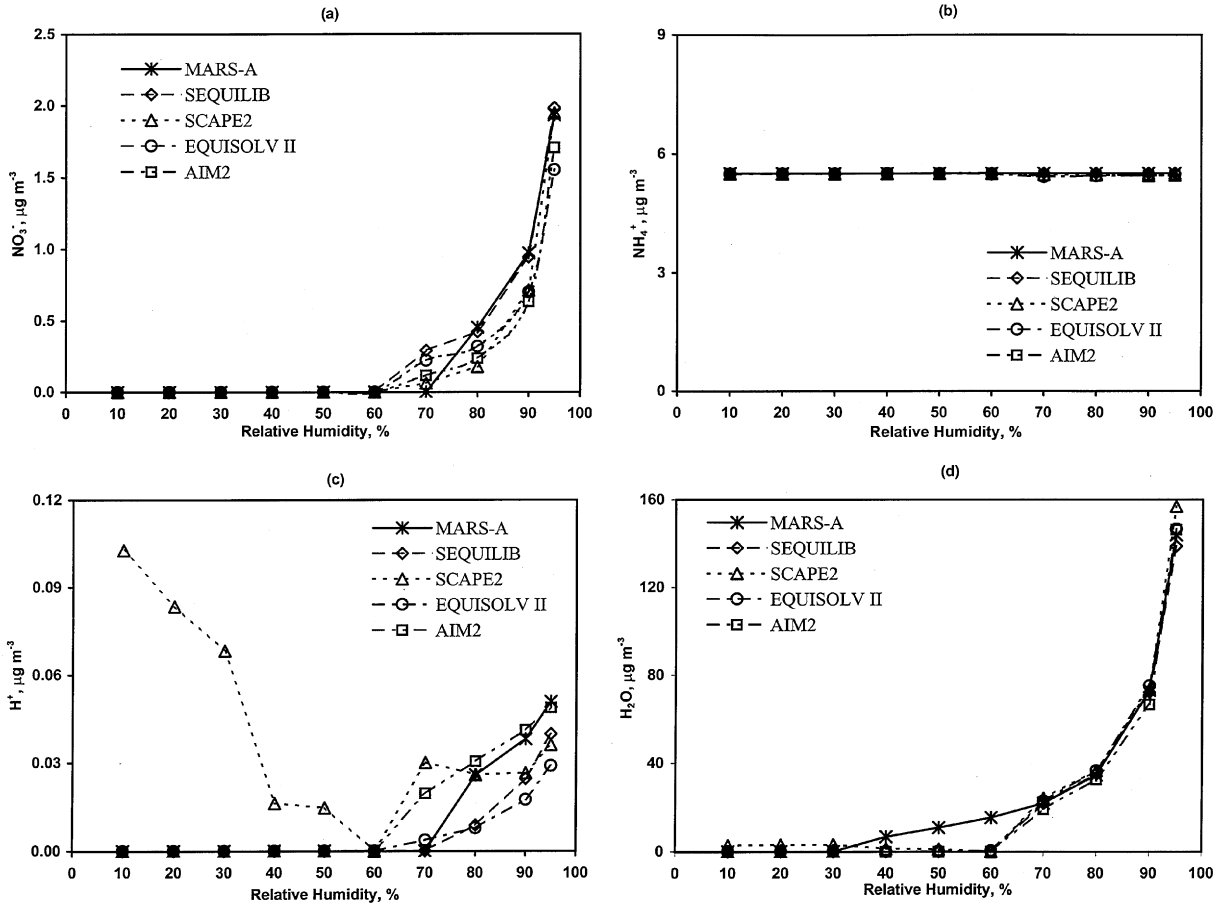

Fig. 2. The concentrations of (a) NO_3^-(p), (b) NH_4^+(p), (c) H^+(p), and (d) H_2O(p) as a function of RH predicted by the five modules at a temperature of 298.15 K under sulfate-rich (i.e., $TNH_4/TSO_4 = 1.5$) conditions.

$[H_2O]_p$ predicted by the five modules are in good agreement for RH > 70%, but show some differences for medium and low RHs. $[H_2O]_p$ predicted by MARS-A are significantly higher than those predicted by other modules for 30% < RH < 70%. This difference is caused by different phase partitioning of relevant species in MARS-A and the other modules. All modules except MARS-A predict particulate sulfate and nitrate species (e.g., $(NH_4)_2SO_4$, $(NH_4)_3H(SO_4)_2$, and NH_4NO_3) to partition between solid and aqueous phases, depending on their deliquescence relative humidities (DRHs) in the multicomponent system. For 30% < RH < 70%, various solid species can exist alone or co-exist with liquid species in these modules. On the other hand, MARS-A does not treat mixed-phase salts, namely, it assumes that various salts are present either in the solid phase or in the aqueous phase, depending on the values of TNH_4/TSO_4 and the assumed crystallization relative humidities (CRHs). For $TNH_4/TSO_4 \geqslant 1$ and RH > 40%, MARS-A predicts that all salts exist in the aqueous phase even though these salts may be present in both solid and aqueous phases. As a result of this assumption, MARS-A predicts much higher electrolytes and water activity, thus, higher $[H_2O]_p$ for 30% < RH < 70%.

Sulfate-neutral and sulfate-poor cases. Under sulfate-neutral and sulfate-poor conditions ($TNH_4/TSO_4 \geqslant 2$), sulfate is fully neutralized as $(NH_4)_2SO_4$ and the system may become alkaline. The excess NH_3(g) drives nitrate from the gas to the particulate phase to form NH_4NO_3 via the NH_3–HNO_3 equilibrium, resulting in the formation of a large amount of NH_4NO_3 for high RHs under both sulfate-neutral and sulfate-poor conditions and precipitation of some NH_4NO_3(s) for low RHs under sulfate-poor conditions. Fig. 3 shows $[NO_3^-]_p$ predicted by the five modules under sulfate-neutral (i.e., $TNH_4/TSO_4 = 2$) and sulfate-poor (i.e., $TNH_4/TSO_4 = 4$) conditions.

For $TNH_4/TSO_4 = 2$, $[NO_3^-]_p$ are negligible for RH ⩽ 60–70%. $[NO_3^-]_p$ predicted by all modules except SEQUILIB significantly increase with RH for higher

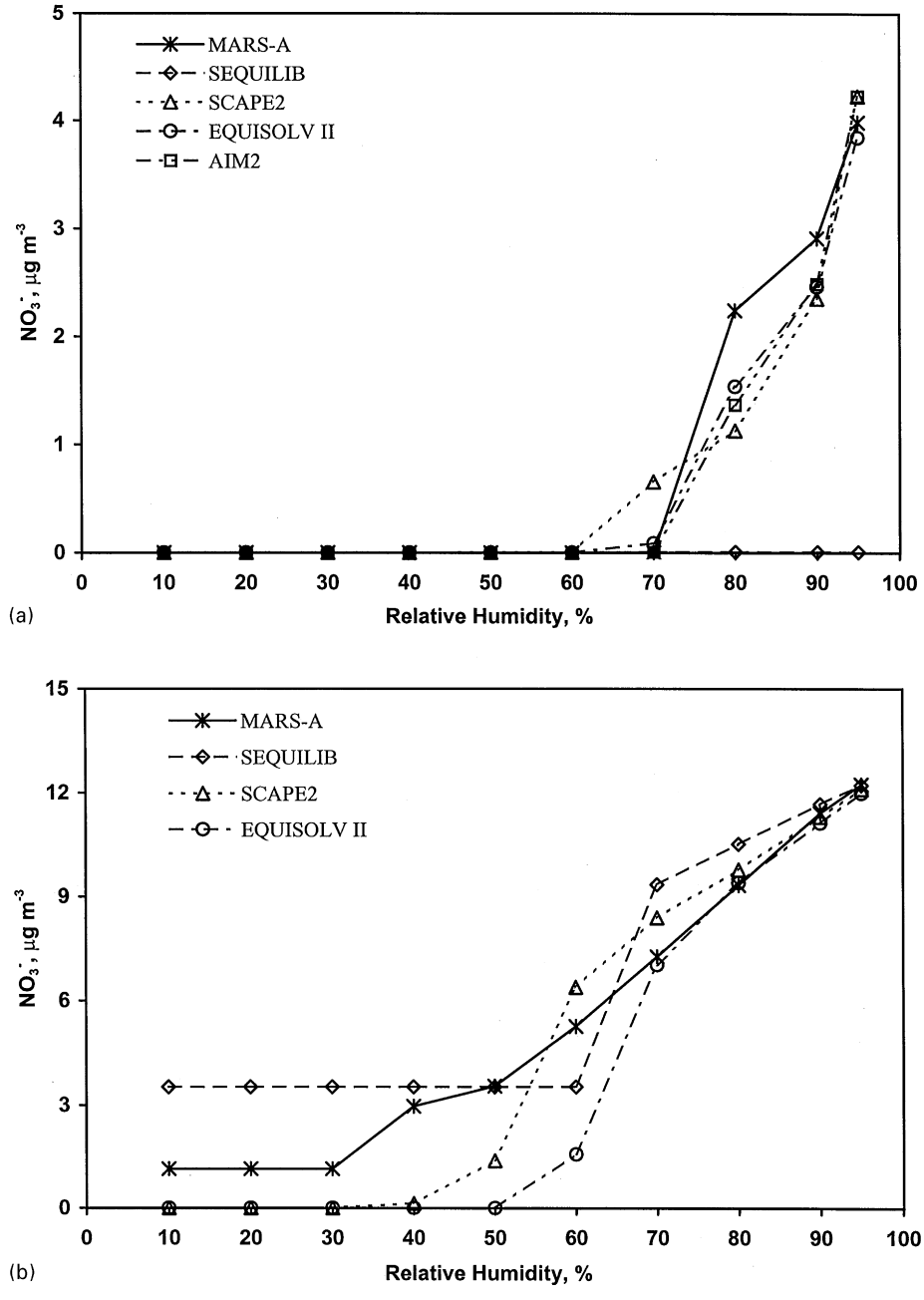

Fig. 3. The concentrations of NO_3^-(p) as a function of RH predicted by the five modules at a temperature of 298.15 K under (a) sulfate-neutral (i.e., $TNH_4/TSO_4 = 2$), and (b) sulfate-poor (i.e., $TNH_4/TSO_4 = 4$) conditions.

RHs (up to 4.5 μg m^{-3}), as more HNO_3 dissolves and dissociates in the aqueous particles. By contrast, $[NO_3^-]_p$ predicted by SEQUILIB becomes negligible (which was non-negligible at RH > 70% for $TNH_4/TSO_4 = 1.5$). This is due to a simplified treatment used in SEQUILIB, which assumes no excess NH_3(g) exists (thus no NH_4NO_3 formation) for $TNH_4/TSO_4 = 2$.

For $TNH_4/TSO_4 = 4$, the system is alkaline and the excess NH_3(g) results in substantial increases in concentrations of NH_4NO_3 (up to 12 μgm^{-3}) for high RHs in all modules except AIM2 (AIM2 does not simulate alkaline systems). Some NH_4NO_3 precipitates for low RHs in MARS-A and SEQUILIB. For RH < 70%, $[NO_3^-]_p$ predicted by the four modules show significant

discrepancies; agreement between them improves as RH increases. The dissociation equilibrium constant for $NH_4NO_3(s) \Leftrightarrow NH_3(g) + HNO_3(g)$ at 298.15 K in MARS-A and in SEQUILIB are about 27 and 48%, respectively, lower than that used in SCAPE2 and EQUISOLV II (see Table 2). These lower equilibrium constants result in lower $NH_3(g)$ and $HNO_3(g)$ thus higher $[NO_3^-]_p$ in both MARS-A and SEQUILIB than SCAPE2 and EQUISOLV II for RH < 50%. There are large differences in $[NO_3^-]_p$ predicted by SCAPE2 and EQUISOLV II for 40% < RH < 80%. This can be attributed to two major reasons. First, NH_3/NH_4^+ equilibria treated in the two modules are different. EQUISOLV II offers the options to include the solid-gas and/or the solid-liquid equilibria of $NH_4Cl(s)$ and $NH_4NO_3(s)$ (i.e., E9, E13, E17, and E18, Table 2). The results of EQUISOLV II were obtained by only turning on E17 and E18. On the other hand, SCAPE2 only treats the solid-gas equilibria of $NH_4Cl(s)$ and $NH_4NO_3(s)$ (i.e., E9 and E13). Second, activity coefficients for some relevant ion pairs used in the two modules are different. In EQUISOLV II, the binary activity coefficients are based on either measurement data or published parameters, whereas in SCAPE2, the binary activity coefficients for some ion pairs (e.g., for NH_4^+/OH^- ion pair) are assumed to be 1.

The PM composition predicted by the five modules under some conditions differs significantly. Fig. 4 shows the predicted PM composition for $TNH_4/TSO_4 = 2$ and RH = 70%. Under this condition, MARS-A, SEQUILIB, and SCAPE2 predict no solid formation, whereas EQUISOLV II and AIM2 predict 23–27 $\mu g\,m^{-3}$ of $(NH_4)_2SO_4(s)$. Since $[H_2O]_p$ is a strong function of electrolyte molality (i.e., the moles of cations and anions per kg of solution) for a given RH (< 100%), the differences in PM composition and molality lead to 23–25 $\mu g\,m^{-3}$ of $H_2O(p)$ formed in MARS-A, SEQUILIB, and SCAPE2 but only 1–4 $\mu g\,m^{-3}$ of $H_2O(p)$ formed in EQUISOLV II and AIM2.

3.3.2. The H^+–Na^+–NH_4^+–NO_3^-–SO_4^{2-}–Cl^-–H_2O System

The presence of NaCl reduces the acidity and increases water content in the particle, causing significant changes in thermodynamic equilibria in the system. Differences in the simulation results for systems containing NaCl among the four modules (MARS-A does not treat NaCl) are generally greater than those without NaCl. Most significant changes occur in the aforementioned sulfate-rich and sulfate-neutral systems because they become sulfate-neutral and sulfate-poor conditions, respectively. In particular, $[Cl^-]_p$ predicted by these modules exhibit significant differences.

Fig. 5(a) shows $[Cl^-]_p$ predicted by the four modules for $TNH_4/TSO_4 = 4$. For RH < 50%, no $Cl^-(p)$ is formed in SEQUILIB, SCAPE2, and AIM2 but $NH_4Cl(s)$ can be formed in EQUISOLV II. No NaCl(s) can be

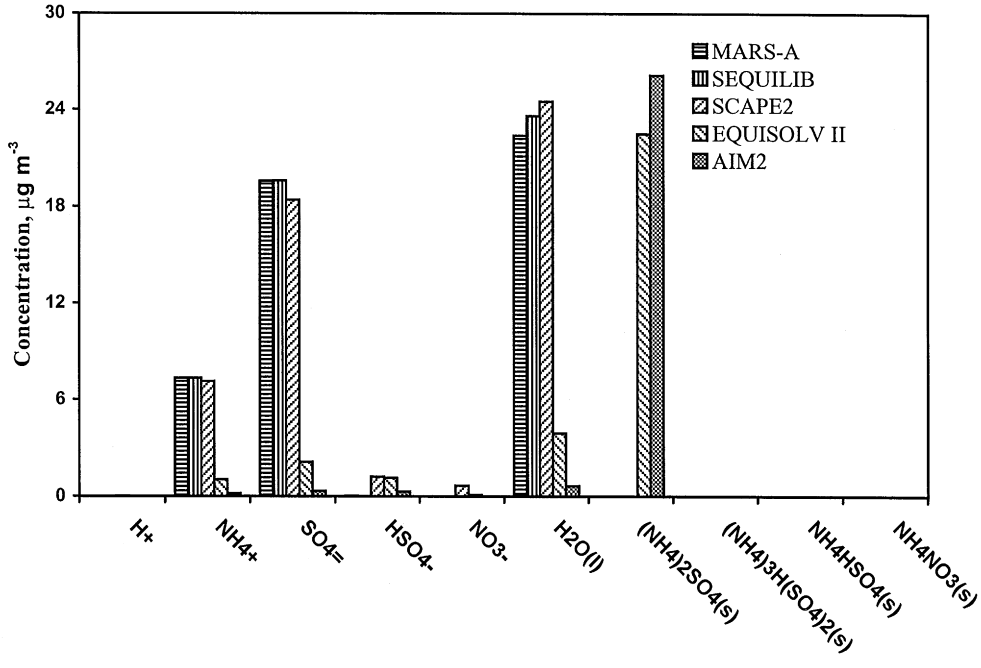

Fig. 4. The PM chemical composition at RH = 70% predicted by the five modules at a temperature of 298.15 K under sulfate-neutral (i.e., $TNH_4/TSO_4 = 2$) conditions.

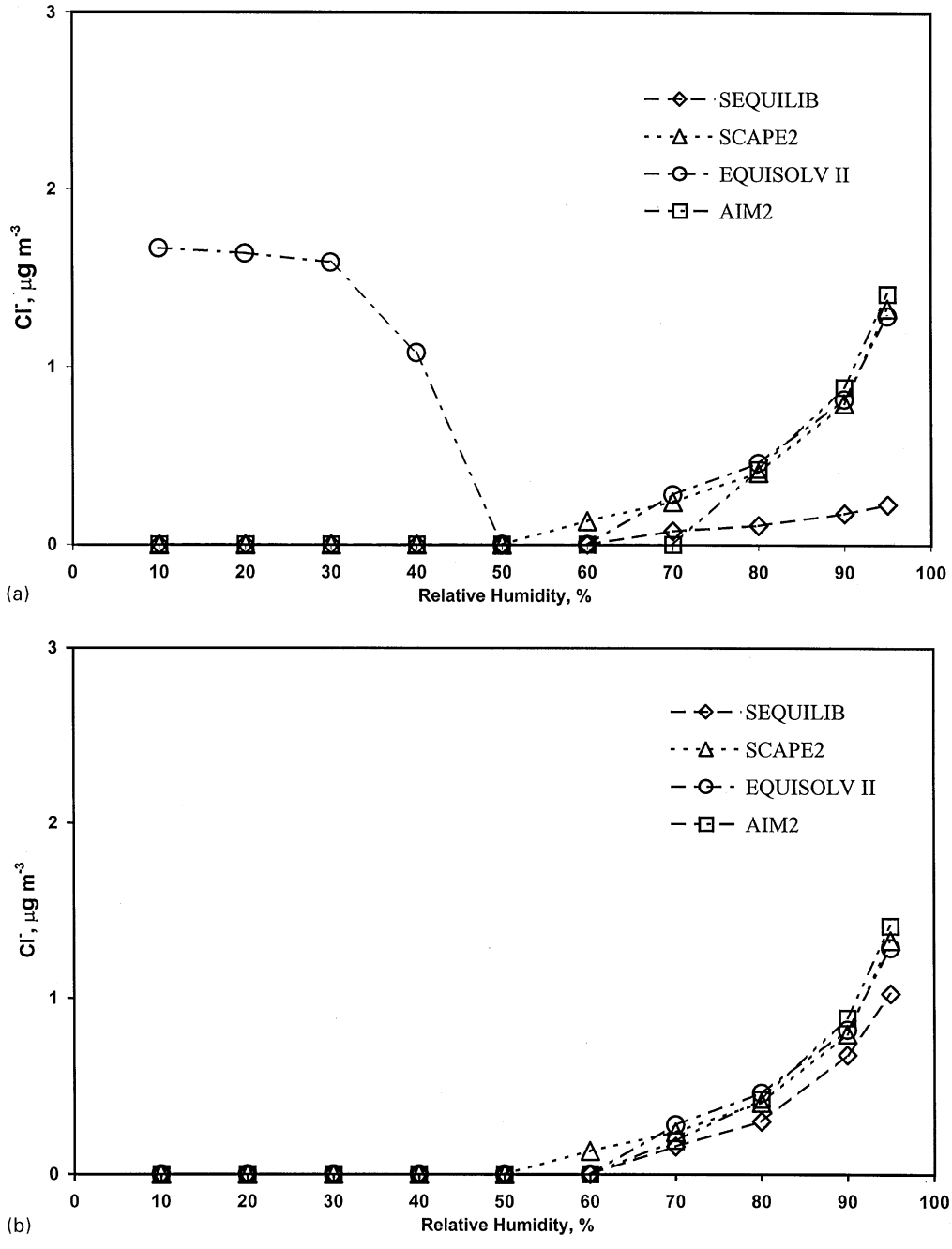

Fig. 5. The concentrations of Cl^-(p) predicted by SEQUILIB, SCAPE2, EQUISOLV II, and AIM2 at a temperature of 298.15 K for the sulfate-poor system with $TNH_4/TSO_4 = 2$, $TNO_3/TSO_4 = 1$, and $TNaCl/TSO_4 = 0.5$ using (a) the original formulation, (b) a set of reactions similar to that used in SCAPE2.

formed under these conditions in all modules. For RH $\geqslant$ 50%, $[Cl^-]_p$ predicted by SCAPE2, EQUISOLV II, and AIM2 are comparable but SEQUILIB predicts significantly lower $[Cl^-]_p$ (by a factor of 2–5) than the other modules. The significant differences in total $[Cl^-]_p$ predicted by these modules can be attributed to different sets of reactions for NH_4NO_3, NH_4Cl, and their dissociated ions. The most important reactions affecting the equilibria of NH_4Cl and NH_4NO_3 include E3–E6, E9, E13, and E17–E20. NH_3(g), HNO_3(g), and HCl(g) dissolve in the solution to form ionic species through equilibria E3–E6 and E19–E20 given sufficient liquid

water (e.g., for RHs greater than DRHs of NH_4NO_3(s), 62%, and NH_4Cl(s), 80%, or supersaturation). Under certain conditions (e.g., when RH decreases), these ions may precipitate to form NH_4Cl(s) and NH_4NO_3(s) via E17–E18. Under low RHs, E9 and E13 can also directly lead to either the formation of NH_4Cl(s) and NH_4NO_3(s) from heterogeneous reactions of NH_3(g) with HCl(g) and HNO_3(g) on the particle or the release of NH_3(g), HCl(g), and HNO_3(g) from NH_4Cl(s) and NH_4NO_3(s).

SEQUILIB includes E5, E6, E19, and E20 and the solid–gas equilibria of NH_4Cl(s) and NH_4NO_3(s) (i.e., E9 and E13). SCAPE2 includes E3, E4a, E5, E6, E9, and E13. EQUISOLV II includes E5, E6, and E19, the solid–liquid and the solid–gas equilibria of NH_4Cl(s) and NH_4NO_3(s) (i.e., E9, E13, E17, and E18) but offers the options to turn on/off individual reactions. The results of EQUISOLV II shown in Fig. 5(a) were obtained by turning on E17 and E18 and turning off E9 and E13. AIM2 simulates E4b, E5, E6, E9, E13, E17–E20 and the solid–liquid equilibria of double salts involving ammonium and nitrate, E23–E25.

Although it is a formidable task to make chemical species and equilibrium reactions identical in these modules due to their different formulations, we conducted additional simulations of SEQUILIB, EQUISOLV II, and AIM2 using a set of reactions similar to that used in SCAPE2 and the results are shown in Fig. 5(b). When E19 is turned off and the equilibrium constants of E6 and E13 were set to be the same values as those in SCAPE2, SEQUILIB can predict $[Cl^-]_p$ that are much closer to those predicted by SCAPE2 under high RHs. When E9 and E13 are turned on, EQUISOLV II yields results similar to those of the other three modules, i.e., no precipitation of NH_4Cl(s) under low RHs. AIM2 also predicts $[Cl^-]_p$ that are much closer to those predicted by the other three modules for $60\% < RH < 80\%$ when all equilibria involving complex salts such as E23–E25 are turned off. $[Cl^-]_p$ predicted by all the four modules agree within 36% for most RHs if a similar set of reactions is used in these modules. In addition, results of EQUISOLV II using both the different and similar sets of reactions show that the solid–gas equilibria E9 and E13 dominate in the system. They favor the release of NH_3(g), HNO_3(g), and HCl(g), resulting in no NH_4Cl(s) formation under low RH conditions.

It is not clear which of these reactions will likely occur and dominate under typical atmospheric ambient PM conditions. It is likely that NH_4^+ and Cl^- ions can precipitate to form NH_4Cl(s) through E17 under certain low and medium RHs when present alone in the particle since the DRH of NH_4Cl(s) is 80%. However, it is an open question whether NH_4Cl(s) can precipitate in particles containing multiple salts under such conditions. Laboratory data are urgently needed to resolve this issue and to provide guidance for improvements in the formulation of thermodynamic equilibrium modules.

3.3.3. Sensitivity of PM predictions

3.3.3.1. Effect of the ratio of total nitrate to total sulfate, TNO_3/TSO_4. In the eastern US, the total nitrate concentrations are usually less than the total sulfate concentrations, while they are generally greater than the total sulfate concentrations in the western US. TNO_3/TSO_4 affects the thermodynamic equilibrium between the gas and particulate phases and the differences in the PM composition predicted by these modules.

For the sulfate-rich systems, the simulation results predicted by the five modules are insensitive or moderately sensitive to the values of TNO_3/TSO_4 because the concentrations of NH_4NO_3 are small and sulfate salts are predominant. The PM predictions are generally comparable for the sulfate-rich systems. The sensitivity of these modules to the values of TNO_3/TSO_4 increases significantly for the sulfate-poor system, in which the excess gaseous ammonia and nitric acid drive NH_3(g) and HNO_3(g) from the gas phase to the particulate phase to form a large amount of NH_4NO_3. Significant discrepancies exist and increase when the values of TNH_4/TSO_4 and TNO_3/TSO_4 increase for the sulfate-poor conditions, under which the effects of different formulations in these modules become much more appreciable than under the sulfate-rich conditions.

As a consequence of changes in PM compositions and their concentrations when TNO_3/TSO_4 varies, the predicted total PM concentrations also increase with TNO_3/TSO_4, especially for high RHs. For the sulfate-rich systems with $TNH_4/TSO_4 = 1.5$ and $RH = 95\%$, the total PM concentrations predicted by MARS-A are insensitive to changes in TNO_3/TSO_4. The other four modules predict similar moderate sensitivity to changes in TNO_3/TSO_4, i.e., the total PM concentrations increase by 19–28% when TNO_3/TSO_4 increases from 0.33 to 3. For the sulfate-poor systems with $TNH_4/TSO_4 = 4$ and $RH = 95\%$, the sensitivity of total PM concentrations predicted by all modules except AIM2 (AIM2 does not simulate alkaline systems) increases significantly. The total PM concentrations increase by 89–123% when TNO_3/TSO_4 varies from 0.33 to 3.

3.3.3.2. Effect of the ratio of total sodium chloride to total sulfate, $TNaCl/TSO_4$. The presence of NaCl can cause dramatic changes in the systems considered here. For the sulfate-rich system, the neutralization of sulfate and nitrate can be greatly enhanced through formation of Na_2SO_4 and/or $NaNO_3$ in the presence of Na^+ ion. As a result, the acidity is reduced and the concentrations of electrolytes and water increase significantly. For the sulfate-poor system, the alkalinity of the system further increases and the excess NH_3(g) can be neutralized by Cl^- ion to form NH_4Cl, resulting in higher concentrations of electrolytes and water. The differences in predicted PM compositions and their

Table 4
Total PM concentrations predicted at 298.15 K and RH = 30% under all conditions[a]

Condition	PM concentrations ($\mu g\ m^{-3}$)					Absolute differences, %				
	MARS-A	SEQUILIB	SCAPE2	EQUISOLV II	AIM2	$\left(\frac{(M-SC)*100}{SC}\right)$	$\left(\frac{(SE-SC)*100}{SC}\right)$	$\left(\frac{2(E-SC)*100}{(E+SC)}\right)$	$\left(\frac{2(A-SC)*100}{(A+SC)}\right)$	$\left(\frac{2(A-E)*100}{(A+E)}\right)$
1	34.2	30.5	34.7	33.0	33.0	− 1.5	− 12.3	− 5.0	− 5.1	− 0.1
2	28.4	23.3	30.3	23.3	23.3	− 6.1	− 23.1	− 26.1	− 26.3	− 0.2
3	25.1	25.1	28.2	25.1	25.1	− 11.1	− 11.1	− 11.6	− 11.6	0.0
4	26.9	26.9	26.9	26.8	26.9	0.0	0.0	− 0.2	− 0.1	0.1
5	28.4	31.5	26.9	26.9	—	5.5	16.9	0.2	—	—
6	25.1	25.1	28.2	25.1	25.1	− 11.1	− 11.1	− 11.7	− 11.6	0.0
7	26.9	26.9	26.9	26.9	—	0.0	0.0	0.2	—	—
8	25.1	25.1	28.2	25.1	25.1	− 11.1	− 11.2	− 11.6	− 11.6	0.0
9	44.7	47.8	41.7	40.5	47.3	7.4	14.7	− 3.0	12.6	15.7
10	—	26.9	27.5	21.5	23.3	—	− 2.1	− 24.6	− 16.7	8.0
11	—	23.3	26.7	23.3	23.3	—	− 12.9	− 13.8	− 13.8	0.0
12	—	25.1	25.1	25.5	25.0	—	0.0	1.6	− 0.2	− 1.8
13	—	26.2	25.1	27.4	25.1	—	4.4	8.7	0.0	− 8.7
14	—	31.7	26.0	30.5	—	—	21.7	15.9	—	—
15	—	25.1	25.1	25.6	25.0	—	0.0	2.1	− 0.2	− 2.3
16	—	26.2	25.1	30.6	—	—	4.4	19.7	—	—
17	—	25.1	25.1	24.9	25.0	—	0.0	− 0.9	− 0.2	0.7
18	—	49.3	44.9	44.1	49.6	—	9.8	− 1.7	9.9	11.6
19	—	24.0	19.6	31.0	19.6	—	22.7	45.2	− 0.1	− 45.2
20	—	32.0	30.2	40.6	—	—	6.1	29.4	—	—

[a]The conditions correspond to those in Table 3. SCAPE2 is used as a reference for MARS-A and SEQUILIB, the percent absolute differences between MARS-A and SCAPE2 and between SEQUILIB and SCAPE2 are $((M - SC)*100/SC)$ and $((SE - SC)*100/SC)$, respectively. For each pair of the three modules: SCAPE2, EQUISOLV-II, and AIM2, the arithmetic averages of values predicted by each pair of modules are used as reference. The normalized absolute percent differences are $(2(E - SC)*100/(E + SC))$ between EQUISOLV II and SCAPE2, $(2(A - SC)*100/(A + SC))$ between AIM2 and SCAPE2, and $(2(A - E)*100/(A + E))$ between AIM2 and EQUISOLV II. MARS-A does not simulate systems containing sodium chloride (i.e., conditions 10–20). AIM2 does not simulate alkaline systems (i.e., conditions 5, 7, 14, 16 and 20).

concentrations also increase significantly when TNaCl/TSO_4 increases.

The changes in PM compositions and concentrations cause corresponding changes in total PM concentrations when TNaCl/TSO_4 varies. For the ammonium-poor system with $TNH_4/TSO_4 = 1.5$ and RH = 95%, the PM concentrations predicted by SEQUILIB are only slightly sensitive to changes in TNaCl/TSO_4. However, the PM concentrations predicted by the other modules are highly sensitive to changes in TNaCl/TSO_4, especially for TNaCl/$TSO_4 = 2$. The total PM concentrations increase by 107–120% as TNaCl/TSO_4 varies from 0 to 2. For the ammonium-rich system with $TNH_4/TSO_4 = 4$ and RH = 95%, the PM concentrations predicted by the three modules (SEQUILIB, SCAPE2, and EQUISOLV II) are also highly sensitive to changes in TNaCl/TSO_4, with an increase by 79–105% when TNaCl/TSO_4 increases from 0 to 2.

3.3.3.3. Effect of temperature. Temperatures affect the PM predictions through changing many properties of the system such as equilibrium constants and activity coefficients. For example, at high temperatures, nitrate salts and liquid water evaporate from the particle, reducing the total PM concentrations. While AIM2 (i.e., AIM2-Model III) is restricted to a fixed temperature of 298.15 K, the temperature dependence of chemical properties is taken into account in the other four modules, as shown in Table 1. The responses of various modules to changes in temperature may be different due to different temperature parameterizations. The discrepancies among modules in the predicted PM compositions likely increase under higher temperatures due to the evaporation of water and semi-volatile species (e.g., nitrate and organic compounds).

Temperature has a significant impact on PM concentrations for the sulfate-poor system, especially for systems with high ammonium and nitrate. For cases with $TNH_4/TSO_4 = 4$, $TNO_3/TSO_4 = 3$, and RH = 60%, when the temperature increases from 298.15 to 308.15 K, the total $[NO_3^-]_p$ predicted by MARS-A, SEQUILIB, SCAPE2, and EQUISOLV II decrease by 79–100%. SEQUILIB predicts zero $[H_2O]_p$ at 298.15 and 308.15 K, and $[H_2O]_p$ predicted by MARS-A, SCAPE2, and EQUISOLV II decrease by 26, 65, and 100%, respectively. The total PM concentrations predicted by the four modules at 308.15 K decrease by 31–55%, as compared to those at 298.15 K. The maximum decrease in total PM concentrations under all modeled conditions is 40% in MARS-A, 56% in SEQUILIB, 63% in SCAPE2, and 78% in EQUISOLV II when the temperature increases from 298.15 to 308.15 K.

3.3.4. Total PM concentrations

Table 4 presents the total PM concentrations predicted by the five modules under all simulation conditions at 298.15 K. RH was assumed to be 30%, consistent with the Federal Reference Method (FRM) for PM measurements. For the ammonium/nitrate/sulfate/water system, the absolute differences between the values predicted by MARS-A and SCAPE2, and by SEQUILIB and SCAPE2 are 6 and 11.2% on average, respectively, ranging from 0 to 11.1% and 0 to 23.1% for specific cases, respectively. The normalized absolute differences between SCAPE2 and EQUISOLV II, between AIM2 and SCAPE2, and between AIM2 and EQUISOLV II are 7.7, 11.3 and 2.3% on average, respectively, ranging from 0.2 to 26.1, 0.1 to 26.3, and 0 to 15.7% for specific cases, respectively. For the sodium/ammonium/nitrate/sulfate/chloride/water system, the absolute difference between the values predicted by SEQUILIB and SCAPE2 is 7.6% on average, ranging from 0 to 22.7% for specific cases. The normalized absolute differences between SCAPE2 and EQUISOLV II, between AIM2 and SCAPE2, and between AIM2 and EQUISOLV II are 14.9, 5.1, and 9.8% on average, respectively, ranging from 0.9 to 45.2, 0 to 16.7, and 0 to 45.2% for specific cases. At 308.15 K, the absolute differences between these modules are similar to those at 298.15 K.

When a similar set of reactions is used in SEQUILIB, SCAPE2, EQUISOLV II, and AIM2, the agreement in the PM concentrations predicted by these modules can be improved, particularly for systems containing NaCl. For the ammonium/nitrate/sulfate/water system, the absolute difference between the values predicted by SEQUILIB and SCAPE2 is 7.8% on average, respectively, ranging from 0 to 23.1% for specific cases. The normalized absolute differences between SCAPE2 and EQUISOLV II, between AIM2 and SCAPE2, and between AIM2 and EQUISOLV II are 7.4, 10.3, and 1.0% on average, ranging from 0.2 to 26.1, 0 to 26.1, and 0 to 6.7% for specific cases, respectively. For the sodium/ammonium/nitrate/sulfate/chloride/water system, the absolute difference between the values predicted by SEQUILIB and SCAPE2 is 5.8% on average, ranging from 0 to 22.4% for specific cases. The normalized absolute differences between SCAPE2 and EQUISOLV II, between AIM2 and SCAPE2, and between AIM2 and EQUISOLV II are 14.2, 4.7, and 2.2% on average, respectively, ranging from 0 to 24.5, 0 to 16.5, and 0 to 8.0% for specific cases.

3.3.5. Timing tests

The time to solve equilibrium equations depends on many factors including the number of equilibrium equations, the method used to solve these equations, and the values of error tolerances. In addition, for a given aerosol module, the computing time varies depending on the case simulated.

We compared the computing times required by the five modules for the 10 case simulations under condition

1 with 10 different RHs here. In these simulations, the numbers of equations that were solved by each module are 7 in MARS-A, 14 in SEQUILIB, 15 in SCAPE2 and EQUISOLV II, and 18 in AIM2. MARS-A uses convergence criteria of 10^{-5} and 10^{-3} for ammonium-rich and ammonium-poor cases, respectively. SEQUILIB uses a convergence criterion of 10^{-2}. SCAPE2 uses convergence criteria of 10^{-7} for H^+ ion and water content calculations and 10^{-2} for solid calculations; the default maximum iteration number is 20. EQUISOLV II uses a normalized gross error in gas and liquid water concentrations of 10^{-4}. AIM2 determines the minimum in the Gibbs energy of the system to about 1 part in 10^{30}. For EQUISOLV II, the same equations were solved for two scenarios: (1) for a single grid cell and (2) for 490 grid cells (for scenario (2), the total CPU time was then divided by 490 to obtain the time to solve in one grid cell). These two scenarios were studied because EQUISOLV II uses a vectorized approach for computations and, therefore, becomes more computationally efficient when the number of grid cells increases. MARS-A, SEQUILIB, SCAPE2, and EQUISOLV II were run on a Compaq Deskpro 2000 with 64 MB RAM, and AIM2 was run on a DEC Alpha 3000 model 600. Single precision was used for all MARS-A, SEQUILIB, and SCAPE2 simulations, double precision was used for all EQUISOLV II simulations. In AIM2, extended (quadruple) precision was used in order to obtain accurate values of the partial pressures of the trace gases, which contribute only a very small amount to the total Gibbs energy of the system.

For the simulation of one case, MARS-A and SEQUILIB used 0.11 and 0.16 s, respectively. SCAPE2 used total times ranging from 0.11 to 0.33 s. EQUISOLV II used total times ranging from 1.81 to 2.9 s for scenario (1) with a single cell and total times ranging from less than 0.01 to 0.17 s for scenario (2) with 490 cells. AIM2 used total times ranging from 1.14 to 3.17 s. SCAPE2, EQUISOLV II, and AIM2 ran faster for high RHs than for low RHs because fewer iterations were needed for high RHs (i.e., fewer solutes and no solids). For a simulation in a single cell, MARS-A, SEQUILIB, and SCAPE2 are generally more computationally efficient than EQUISOLV II and AIM2 (faster by a factor of 7–29). Note, however, that the total CPU time for the simulation of one case by AIM2 can be faster by a factor of 10 if an ordinary double precision is used. As the number of grid cells simulated increases, EQUISOLV II is generally more computationally efficient than the other four modules, with a factor of 2–20 faster than MARS-A, SEQUILIB, and SCAPE2, and a factor of 19–243 faster than AIM2.

The difference in program speed is due to the differences in the numerical methods and calculation procedures in these modules. In particular, MARS-A uses an analytical method and a subdomain approach for PM calculations in different thermodynamic regimes. SEQUILIB and SCAPE2 also use the subdomain approach. SEQUILIB uses a method combining the iterative bisectional and Newton–Raphson methods and SCAPE2 uses the iterative bisectional method. Both methods can rapidly converge mass and charge for most systems in a box model. However, they may require extensive iterations for some systems with highly acidic particles and may result in small negative concentrations when a large number of iterations are used. For example, SCAPE2 solved the equations for the simulation for RH $= 30\%$ using a CPU three times longer (i.e., 0.33 s) than those for high RH cases, but the solution still did not converge. A convergence solution for this case can be obtained by increasing the iteration number from 20 to 100, but the CPU also increases proportionally (i.e., by a factor of 5). When a maximum number of iterations of 500 was used, SCAPE2 predicted small negative concentrations of particulate nitrate in three cases out of 200 cases. EQUISOLV II solves all equations for all thermodynamic regimes using a hybrid MFI/AEI scheme, which requires relatively large CPU time to solve equations in one grid cell but speeds up significantly for simulations for multiple grid cells. The computational speed of EQUISOLV II improves with increasing number of grid cells because all inner loops are vectorized around the grid cell dimension array. On a scalar machine, this results in a number of array references that is constant, regardless of the number of grid cells in a grid block (group of many cells). Thus, when the number of grid cells increases, the computer time required per grid cell decreases. On a vector machine, additional speed increases occur with multiple cells due to the vectorization. AIM2 solves all equations for all thermodynamic regimes using the sequential quadratic programming algorithm to minimize the Gibbs free energy of the system. The computational speed of AIM2 is relatively slow, due mainly to the computational cost for calculations of activity coefficients and the use of an extended precision. Although the version of AIM2 used in this work has not been programmed for the purpose of inclusion in a 3-D model, its computational speed can be greatly improved for such a 3-D application.

4. Conclusions and recommendations

We have conducted a comprehensive evaluation of five aerosol thermodynamic equilibrium modules under a variety of atmospheric PM concentrations, RHs, and temperatures. Although the PM predictions of these modules are generally comparable under most conditions, significant discrepancies exist under some conditions, especially under high nitrate/chloride concentrations and low/medium RH conditions. The normalized absolute differences in total PM concentrations predicted by the

five modules under all conditions and a temperature of 298.15 K are 7.7–12.3%. The differences can be as much as 68% for specific cases. For RH = 30% (i.e., conditions typical of FRM measurements) under typical ambient temperatures (298.15–308.15 K), the PM concentrations predicted by the five modules differ by 4–13% on average and by as much as 63% for specific cases. The PM compositions and concentrations predicted by the five modules are highly sensitive to changes in the molar ratios of ammonium to sulfate, nitrate to sulfate, and sodium chloride to sulfate, RH, and temperature. The differences in PM predictions are due mainly to differences in the chemical species and equilibrium reactions that are treated, the values of the equilibrium constants, the computational procedures and associated assumptions, and the methods used to calculate binary and multi-component activity coefficients and water activities. The differences in the temperature parameterizations seem to have little effects on the differences in PM predictions among these modules under most conditions modeled in this study.

MARS-A predicted higher $[H_2O]_p$ for medium RHs than other modules due mainly to its assumption that no solid exists for medium RHs. For some conditions tested here, SEQUILIB predicts abnormal $[NO_3^-]_p$ and $[H^+]_p$ due to numerical errors and lower $[Cl^-]_p$ than those predicted by the other modules due to a different set of equilibrium reactions used in SEQUILIB. Both MARS-A and SEQUILIB predict higher NH_4NO_3 for most cases than the other modules due to differences in the relevant equilibrium constants used and/or differences and assumptions in thermodynamic treatment. SCAPE2 predicts higher $[H^+]_p$ for highly concentrated particles (i.e., under sulfate-rich and low RH conditions) due to numerical artifacts caused by non convergence of the solution. EQUISOLV II predicts higher NH_4Cl for cases with NaCl and low RHs due to different equilibrium reactions used for NH_4Cl and NH_4NO_3. AIM2 predicts results comparable to those predicted by the other modules for most acidic systems but does not simulate alkaline systems. The differences in PM predictions between AIM2 and the other modules are mainly due to the treatments of additional equilibrium reactions involving complex salts and different methods to calculate activity coefficients. Our results also show that the differences among the five modules can be greatly minimized by using a similar set of equilibrium reactions in these modules.

Ansari and Pandis (1999b) compared four aerosol thermodynamic modules: GFEMN, ISORROPIA, SCAPE2, and SEQUILIB under marine, remote continental, and non-urban continental conditions. They found that the normalized mean errors between the most accurate module GFEMN and the other three modules are 13–26% for $[NO_3^-]_p$ and 39–256% for $[H_2O]_p$ under sulfate-poor conditions and 22–52% for $[NH_4^+]_p$, 403–1134% for $[H^+]_p$, and 25–82% for $[H_2O]_p$ under sulfate-rich conditions. Among these modules, SCAPE2 predicted the highest $[H^+]_p$ under sulfate-rich and low RH conditions. Significant discrepancies exist in $[H_2O]_p$ for sulfate-rich conditions and in $[NH_4^+]_p$, $[H_2O]_p$, and total dry PM concentrations (i.e., excluding $[H_2O]_p$) for sulfate-poor conditions between SEQUILIB and the other three modules. Despite these differences, the total dry PM concentrations predicted by ISORROPIA, SCAPE2, and SEQUILIB are in good agreement to those predicted by GFEMN, with a mean normalized error of $< 6\%$. Our comparisons were conducted for typical urban and coastal conditions, with a broader range of RHs, higher concentration of sulfate, and higher concentration ranges of total nitrate, ammonium, and sodium chloride than those of Ansari and Pandis (1999b). Only two modules, SEQUILIB and SCAPE2, are common to both studies. Our results show 8–12% differences among the total PM concentrations (including $[H_2O]_p$) and much larger differences in concentrations of particulate compositions. Overall, our results and those of Ansari and Pandis (1999b) are consistent. The version of SEQUILIB used by Ansari and Pandis (1999b) is a most recent version than that used in this work. Although the most recent version predicts slightly different results than the earlier version, the major discrepancies identified under our test conditions were found to remain the same.

Our results provide useful information for the selection of aerosol thermodynamic equilibrium modules for future PM modeling studies. The selection of a thermodynamic module for 3-D air quality modeling may depend on the specific objectives of the study and it is important to understand the advantages and disadvantages of existing modules before incorporating them into a host air quality model.

Given its simplest chemistry, MARS-A predicts results comparable to those predicted by the other more comprehensive modules under high RH conditions. However, MARS-A does not simulate sodium chloride and assumes a metastable state for the particles. This assumption may not be applicable in dry areas where RH values are very low and the particles may not be in a metastable state. Therefore, caution is advised when applying MARS-A to dry areas (e.g., southwestern US) and coastal areas.

The version of SEQUILIB that is currently used in UAM-AERO and SAQM-AERO should be improved because it gives unstable or even abnormal solutions for PM predictions under many conditions. An improved version of SEQUILIB exists, but it generally does not improve the major discrepancies identified for the urban and coastal conditions selected in this work. Further improvements of SEQUILIB appear warranted.

SCAPE2, EQUISOLV II, and AIM2 contain most comprehensive aerosol chemistry and thermodynamics, providing detailed PM predictions. Both SCAPE2 and

EQUISOLV II can be applied to simulate PM for any conditions, whereas AIM2 can be applied only to acidic systems. The total CPU time is likely proportional to the number of grid cells simulated in SCAPE2 and AIM2, posing computational constraints and challenges for their applications to large domains. On the other hand, the vectorization used in the numerical scheme in EQUISOLV II permits continuous solutions with relatively fast speed over large numbers of spatial grid cells and particle size bins for 3-D PM modeling. However, the computer must have sufficient memory bandwidth (ability to transfer information to and from memory quickly) because the vectorized EQUISOLV II requires more memory than the other non-vectorized codes.

Acknowledgements

This project was supported by the Coordinating Research Council under Contract A-21-2. Y.Z. and C.S. would like to thank Spyros N. Pandis for providing simulations for a few cases using the GFEMN module to help clarify discrepancies between EQUISOLV and the other four modules.

References

Allen, A.G., Harrison, R.M., Erisman, J., 1989. Field measurements of the dissociation of ammonium nitrate and ammonium chloride aerosols. Atmospheric Environment 17, 1591–1599.

Ansari, A.S., Pandis, S.N., 1999a. Prediction of multicomponent inorganic atmospheric aerosol behavior. Atmospheric Environment 33, 745–757.

Ansari, A.S., Pandis, S.N., 1999b. An analysis of four models predicting the partitioning of semi-volatile inorganic aerosol components. Aerosol Science and Technology in press.

Bassett, M.E., Seinfeld, J.H., 1983. Atmospheric equilibrium model of sulfate and nitrate aerosol. Atmospheric Environment 17, 2237–2252.

Bassett, M.E., Seinfeld, J.H., 1984. Atmospheric equilibrium model of sulfate and nitrate aerosol. II, Particle size analysis. Atmospheric Environment 18, 1163–1170.

Binkowski, F.S., Shankar, U., 1995. The regional particulate matter model, 1: model description and preliminary results. Journal of Geophysical Research 100, 26191–26209.

Chan, C.K., Flagan, R.C., Seinfeld, J.H., 1992. Water activities of $NH_4NO_3/(NH_4)_2SO_4$ solutions. Atmospheric Environment 26, 1661–1673.

Clegg, S.L., Brimblecombe, P., Wexler, A.S., 1998a. A thermodynamic model of the system H^+–NH_4^+–Na^+–SO_4^{2-}–NO_3^-–Cl^-–H_2O at 298.15 K. Journal of Physical Chemistry 102, 2155–2171.

Clegg, S.L., Brimblecombe, P., Wexler, A.S., 1998b. A thermodynamic model of the system H^+–NH_4^+–Na^+– SO_4^{2-}–NO_3^-–Cl^-–H_2O at tropospheric temperatures. Journal of Physical Chemistry 102, 2137–2154.

Clegg, S.L., Pitzer, K.S., Brimblecombe, P., 1992. Thermodynamics of multicomponent, miscible, ionic solutions. II. Mixture including unsymmetrical electrolytes. Journal of Physical Chemistry 96, 9470–9479.

Clegg, S.L., Pitzer, K.S., Brimblecombe, P., 1994. (additions and corrections for their published papers). Journal of Physical Chemistry 98, 1368.

Clegg, S.L., Pitzer, K.S., Brimblecombe, P., 1995. (additions and corrections for their published papers). Journal of Physical Chemistry 99, 6755.

Cohen, M.D., Flagan, R.C., Seinfeld, J.H., 1987a. Studies of concentrated electrolyte solutions using the electrodynamic balance – I. Water activities for single-electrolyte solutions. Journal of Physical Chemistry 91, 4563–4574.

Cohen, M.D., Flagan, R.C., Seinfeld, J.H., 1987b. Studies of concentrated electrolyte solutions using the electrodynamic balance – II. Water activities for mixed-electrolyte solutions. Journal of Physical Chemistry 91, 4575–4582.

Dabdub, D., Dehaan, L.L., Kumar, N., Lurmann, F., Seinfeld, J.H., 1997. Computationally efficient acid deposition model for California, draft report for the California Air Resources Board. Sacramento, California.

Gray, H.A., Cass, G.R., Huntzicker, J.J., Heyerdahl, E.K., Rau, J.A., 1986. Characteristics of atmospheric organic and elemental carbon particle concentrations in Los Angeles. Environmental Science and Technology 20, 580–589.

Jacobson, M.Z., Tabazadeh, A., Turco, R.P., 1996a. Simulating equilibrium within aerosols and nonequilibrium between gases and aerosols. Journal of Geophysical Research 101, 9079–9091.

Jacobson, M.Z., Lu, R., Turco, R.P., Toon, O.B., 1996b. Development and application of a new air pollution modeling system. Part I. Gas-phase simulations. Atmospheric Environment 30B, 1939–1963.

Jacobson, M.Z., 1997. Development and application of a new air pollution modeling system – Part II. Aerosol modules structure and design. Atmospheric Environment 31, 131–144.

Jacobson, M.Z., 1999a. Chemical equilibrium and dissolution processes, Fundamentals of Atmospheric Modeling. Cambridge University Press, New York, pp. 476–510 (Chapter 18).

Jacobson, M.Z., 1999b. Studying the effects of calcium and magnesium on size-distributed nitrate and ammonium with EQUISOLV II. Atmospheric Environment 33, 3635–3649.

Kim, Y.P., Seinfeld, J.H., Saxena, P., 1993a. Atmospheric gas aerosol equilibrium, I: thermodynamic model. Aerosol Science and Technology 19, 157–181.

Kim, Y.P., Seinfeld, J.H., Saxena, P., 1993b. Atmospheric gas aerosol equilibrium, II: analysis of common approximations and activity coefficient calculation methods. Aerosol Science and Technology 19, 182–198.

Kim, Y.P., Seinfeld, J.H., 1995. Atmospheric gas-aerosol equilibrium III: thermo-dynamics of crustal elements Ca^{2+}, K^+, and Mg^{2+}. Aerosol Science and Technology 22, 93–110.

Lurmann, F.W., Wexler, A.S., Pandis, S.N., Musarra, S., Kumar, N., Seinfeld, J.H., 1997. Modeling urban and regional aerosols – II. Application to California's south coast air basin. Atmospheric Environment 31, 2695–2715.

Meng, Z., Seinfeld, J.H., Saxena, P., Kim, Y.P., 1995. Atmospheric gas-aerosol equilibrium, IV: thermodynamics of carbonates. Aerosol Science and Technology 23, 131–154.

Meng, Z., Dabdub, D., Seinfeld, J.H., 1998. Size- and chemically-resolved model of atmospheric aerosol dynamics. Journal of Geophysical Research 103, 3419–3435.

Middleton, D., 1997. DAQM – Simulated spatial and temporal differences among visibility, PM and other air quality concerns under realistic emission change scenarios. Journal of Air Waste Management Association 47, 302–316.

Nenes, A., Pilinis, C., Pandis, S.N., 1998. ISORROPIA: a new thermodynamic equilibrium model for multiphase multicomponent marine aerosols. Aquatic Geochemistry 4, 123–152.

Nenes, A., Pilinis, C., Pandis, S.N., 1999. Continued development and testing of a new thermodynamic aerosol module for urban and regional air quality models. Atmospheric Environment 33, 1553–1560.

Pilinis, C., Seinfeld, J.H., 1987. Continued development of a general equilibrium model for inorganic multicomponent atmospheric aerosols. Atmospheric Environment 32, 2453–2466.

Saxena, P., Seigneur, C., Hudischewskyj, A.B., Seinfeld, J.H., 1986. A comparative study of equilibrium approaches to the chemical characterizations of secondary aerosols. Atmospheric Environment 20, 1471–1484.

Sun, Q., Wexler, A.S., 1998. Modeling urban and regional aerosols near acid neutrality – application to the June 24–25 SCAQS episode. Atmospheric Environment 32, 3533–3542.

Wexler, A.S., Seinfeld, J.H., 1990. The distribution of ammonium salts among a size and composition dispersed aerosol. Atmospheric Environment 24A, 1231–1246.

Wexler, A.S., Seinfeld, J.H., 1991. Second-generation inorganic aerosol model. Atmospheric Environment 25A, 2731–2748.